GEOPHYSICS, VOL. 73, NO. 6 (NOVEMBER-DECEMBER 2008); P. A51–A56, 3 FIGS.
10.1190/1.2976118

Passive seismic interferometry by multidimensional deconvolution

Kees Wapenaar[1], Joost van der Neut[1], and Elmer Ruigrok[1]

ABSTRACT

We introduce seismic interferometry of passive data by multidimensional deconvolution (MDD) as an alternative to the crosscorrelation method. Interferometry by MDD has the potential to correct for the effects of source irregularity, assuming the first arrival can be separated from the full response. MDD applications can range from reservoir imaging using microseismicity to crustal imaging with teleseismic data.

INTRODUCTION

Under specific conditions, the crosscorrelation of wavefields observed at two receivers yields the impulse response between these receivers. This principle is known as Green's function retrieval or seismic interferometry. Wapenaar et al. (2008a) and Schuster (Seismic Interferometry, in press) provides an overview of this rapidly expanding field of research.

In many situations, it can be advantageous to replace the correlation process by deconvolution. One of the advantages is that deconvolution compensates for the properties of the source wavelet; another advantage is that it is unnecessary to assume the medium is lossless. Snieder et al. (2006) deconvolve passive wavefields observed at different depth levels and show that this leads to an estimate of the impulse response. They apply it to earthquake data recorded at different heights at Pasadena, California's Millikan library and obtain the impulse response of the building. Mehta et al. (2007) use a similar approach to estimate the near-surface properties of the earth from passive recordings in a vertical borehole. Both approaches employ a 1D deconvolution process.

Various authors have shown that multidimensional deconvolution (MDD), applied to controlled-source data with receivers at a constant depth level (for example, at the ocean bottom or in a horizontal borehole), can obtain the response of a redatumed source without needing a model. Wapenaar and Verschuur (1996) and Amundsen (1999) use MDD of wavefields recorded at the ocean bottom to obtain the response of the subsurface without ocean-bottom and surface-related multiples. Schuster and Zhou (2006) and Wapenaar et al. (2008b) discuss MDD of controlled-source data in the context of seismic interferometry.

In this letter, we propose a method for seismic interferometry of passive data by MDD and show that, under specific circumstances, the method compensates for irregularities in the source distribution. This is an important difference with crosscorrelation methods, which rely on the condition that waves are equipartitioned (Malcolm et al., 2004; Snieder et al., 2007). The condition is fulfilled, for example, when the sources are distributed regularly along a closed surface and the power spectra of the sources are identical. MDD compensates for anisotropic illumination without requiring knowledge about the positions and spectra of the sources.

IMPLICIT GREEN'S FUNCTION REPRESENTATION

We consider an arbitrary inhomogeneous anisotropic dissipative medium in which we define a domain $\mathbb{D}$ enclosed by a boundary $\partial\mathbb{D}$ with outward-pointing normal vector $\mathbf{n} = (n_1, n_2, n_3)$. In the space-frequency $(\mathbf{x}, \omega)$ domain, the Rayleigh-Betti reciprocity theorem for elastodynamic wavefields is given by (Aki and Richards, 1980)

$$\oint_{\partial\mathbb{D}} (\hat{v}_{i,A}\hat{t}_{i,B} - \hat{v}_{j,B}\hat{t}_{j,A})\mathrm{d}^2\mathbf{x} = \int_{\mathbb{D}} (\hat{v}_{k,B}\hat{f}_{k,A} - \hat{v}_{l,A}\hat{f}_{l,B})\mathrm{d}^3\mathbf{x}, \tag{1}$$

where $\hat{v}_i = \hat{v}_i(\mathbf{x}, \omega)$ represents the particle velocity (the circumflex denotes the frequency domain), $\hat{t}_j = \hat{t}_j(\mathbf{x}, \omega)$ is the traction (with $\hat{t}_j = \hat{\tau}_{jp}n_p$, where $\hat{\tau}_{jp}$ is the stress), and $\hat{f}_k = \hat{f}_k(\mathbf{x}, \omega)$ is the external volume force. The lowercase subscripts i, j, etc., take on the values 1, 2, and 3; Einstein's summation convention applies to repeated lowercase subscripts. The uppercase subscripts A and B refer to two independent elastodynamic states. The medium parameters in $\mathbb{D}$ are assumed to be the same in both states; outside $\mathbb{D}$ they may be different,

Manuscript received by the Editor 21 March 2008; revised manuscript received 16 May 2008; published online 16 October 2008.
[1]Delft University of Technology, Department of Geotechnology, Delft, The Netherlands. E-mail: c.p.a.wapenaar@tudelft.nl; j.r.vanderneut@tudelft.nl; e.n.ruigrok@tudelft.nl.

whereas at $\partial\mathbb{D}$ different boundary conditions may apply for the wavefields in states A and B.

Note that the products $\hat{v}_{i,A}\hat{t}_{i,B}$, etc., in the frequency domain correspond to convolutions ($v_{i,A} * t_{i,B}$, etc.) in the time domain. For this reason, we call equation 1 a reciprocity theorem of the convolution type. In previous work, we start with correlation reciprocity theorems, leading to representations for Green's function retrieval by crosscorrelation. Here we use the convolution theorem of equation 1 to derive an implicit representation for Green's function retrieval by MDD.

We let $\partial\mathbb{D}$ consist of $\partial\mathbb{D}_0$, coinciding with the earth's free surface (not necessarily planar), and a hemisphere $\partial\mathbb{D}_1$ with infinite radius in the lower half-space (Figure 1). The contribution of $\partial\mathbb{D}_1$ to the boundary integral in the left-hand side of equation 1 vanishes because of Sommerfeld's radiation condition. If we would take free-surface boundary conditions at $\partial\mathbb{D}_0$ in both states, then the integral over $\partial\mathbb{D}_0$ would vanish as well. To retain a nonzero integral over $\partial\mathbb{D}_0$, we choose different boundary conditions for the wavefields in states A and B at $\partial\mathbb{D}_0$. In state B, we assume free-surface boundary conditions, as in the actual situation (Figure 1b); but in state A, we let $\partial\mathbb{D}_0$ be a transparent surface (Figure 1a).

In state A, we choose a point source of volume force at $\mathbf{x}_A$ somewhere in the lower half-space; hence, $\hat{f}_{k,A}(\mathbf{x},\omega) = \delta_{3D}(\mathbf{x} - \mathbf{x}_A)\hat{s}_k(\mathbf{x}_A,\omega)$, where $\delta_{3D}(\mathbf{x} - \mathbf{x}_A)$ is a 3D Dirac delta function and $\hat{s}_k(\mathbf{x}_A,\omega)$ is the source spectrum. For the wavefield emitted by this

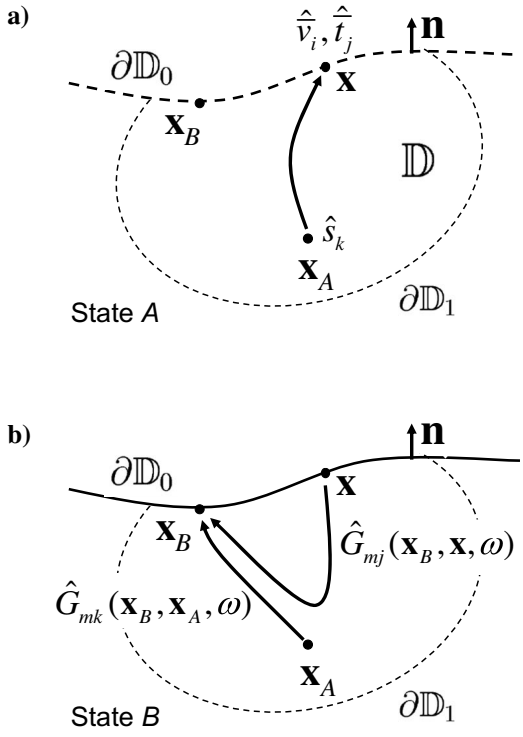

Figure 1. Medium configuration and wavefields in states A and B. In the reference state (A), $\partial\mathbb{D}_0$ is a transparent surface; in the actual state (B), it is a free surface. The rays represent full responses between the indicated source and receiver points, including primary and multiple scattering caused by inhomogeneities of the medium and (in state B) by the free surface. In state A, the source is a point source of volume force at $\mathbf{x}_A$; in state B, it is a point source of surface traction at $\mathbf{x}_B$. The Green's functions shown in state B are the reciprocal versions, with a receiver at $\mathbf{x}_B$.

source, we write $\hat{v}_{i,A}(\mathbf{x},\omega) = \hat{\bar{v}}_i(\mathbf{x},\mathbf{x}_A,\omega)$ and $\hat{t}_{j,A}(\mathbf{x},\omega) = \hat{\bar{t}}_j(\mathbf{x},\mathbf{x}_A,\omega)$, where the bars denote the reference situation with the transparent surface $\partial\mathbb{D}_0$ (see Figure 1a).

In state B, we introduce a source in terms of a boundary condition at the free surface $\partial\mathbb{D}_0$. This is possible because, at a free surface, the traction is zero everywhere except where a source traction is applied. We define a point source of surface traction with unit amplitude in the x_m-direction at $\mathbf{x}_B \in \partial\mathbb{D}_0$, according to $\hat{t}_{i,B}(\mathbf{x},\omega) = \delta_{2D}(\mathbf{x} - \mathbf{x}_B)\delta_{im}$ for $\mathbf{x} \in \partial\mathbb{D}_0$, where $\delta_{2D}(\mathbf{x} - \mathbf{x}_B)$ is a 2D Dirac delta function in $\partial\mathbb{D}_0$ and δ_{im} is the Kronecker delta function. The response of this unit source is expressed in terms of a Green's function, according to $\hat{v}_{j,B}(\mathbf{x},\omega) = \hat{G}_{jm}(\mathbf{x},\mathbf{x}_B,\omega) = \hat{G}_{mj}(\mathbf{x}_B,\mathbf{x},\omega)$. This is the Green's function of the actual medium, including the reflections of the free surface at $\partial\mathbb{D}_0$ (see Figure 1b).

Substituting these sources and wavefields into equation 1, taking $\hat{f}_{l,B}(\mathbf{x},\omega) = 0$, we obtain

$$\int_{\partial\mathbb{D}_0} \hat{G}_{mj}(\mathbf{x}_B,\mathbf{x},\omega)\hat{\bar{t}}_j(\mathbf{x},\mathbf{x}_A,\omega)\mathrm{d}^2\mathbf{x} = -\{\hat{v}_m(\mathbf{x}_B,\mathbf{x}_A,\omega) - \hat{\bar{v}}_m(\mathbf{x}_B,\mathbf{x}_A,\omega)\}, \quad (2)$$

with $\hat{v}_m(\mathbf{x}_B,\mathbf{x}_A,\omega) = \hat{G}_{mk}(\mathbf{x}_B,\mathbf{x}_A,\omega)\hat{s}_k(\mathbf{x}_A,\omega)$ denoting the observed passive data at the free surface, attributable to a source in the subsurface (hence, it can be seen as the transmission response of the medium). The values $\hat{\bar{v}}_m(\mathbf{x}_B,\mathbf{x}_A,\omega)$ and $\hat{\bar{t}}_j(\mathbf{x},\mathbf{x}_A,\omega)$ represent the responses in the reference state of the same subsurface source; under specific conditions (see next section), these can be estimated from the observed data $\hat{v}_m(\mathbf{x}_B,\mathbf{x}_A,\omega)$.

Equation 2 is an implicit representation of the convolution type for the Green's function $\hat{G}_{mj}(\mathbf{x}_B,\mathbf{x},\omega)$ with source and receiver at the free surface $\partial\mathbb{D}_0$ (i.e., the reflection response of the medium, including an integrable singularity for $\mathbf{x} = \mathbf{x}_B$). If it were a single equation, the inverse problem would be ill posed. However, equation 2 exists for each source position $\mathbf{x}_A$ and for each available source component at $\mathbf{x}_A$. Solving this ensemble of equations for $\hat{G}_{mj}(\mathbf{x}_B,\mathbf{x},\omega)$ involves MDD, as we show in the next section.

Although in the derivation we assume a point source of volume force at $\mathbf{x}_A$, a similar derivation shows that equation 2 holds equally well for other types of sources at $\mathbf{x}_A$, such as volume-injection or shear-dislocation sources (e.g., resulting from fault slip). The source also is not necessarily a point source. For an extended source, both sides of equation 2 can be integrated over $\mathbf{x}_A$ along the extended source, yielding an equation with exactly the same form but with $\hat{v}_m$, $\hat{\bar{v}}_m$ and $\hat{\bar{t}}_j$ being the responses of the extended source.

MULTIDIMENSIONAL DECONVOLUTION (MDD)

Here we discuss the solution of equation 2 for the acoustic situation. In a later section, we indicate the required modifications for the elastodynamic situation.

We first define $\hat{\bar{t}}_j(\mathbf{x},\mathbf{x}_A,\omega) = -\delta_{jp}n_p\hat{\bar{p}}(\mathbf{x},\mathbf{x}_A,\omega)$, where $\hat{\bar{p}}$ is the acoustic pressure in the reference state. Substituting into equation 2 and multiplying both sides by $-n_m$ gives

$$\int_{\partial\mathbb{D}_0} \hat{G}(\mathbf{x}_B,\mathbf{x},\omega)\hat{\bar{p}}(\mathbf{x},\mathbf{x}_A,\omega)\mathrm{d}^2\mathbf{x} = \hat{v}(\mathbf{x}_B,\mathbf{x}_A,\omega) - \hat{\bar{v}}(\mathbf{x}_B,\mathbf{x}_A,\omega), \quad (3)$$

where $\hat{v}(\mathbf{x}_B,\mathbf{x}_A,\omega) = n_m\hat{v}_m(\mathbf{x}_B,\mathbf{x}_A,\omega)$ and $\hat{\bar{v}}(\mathbf{x}_B,\mathbf{x}_A,\omega) = n_m\hat{\bar{v}}_m(\mathbf{x}_B,\mathbf{x}_A,\omega)$ are the normal components of the particle velocity in the actual and in the reference states, respectively. Similarly, $\hat{G}(\mathbf{x}_B,\mathbf{x},\omega) = n_m n_j\hat{G}_{mj}(\mathbf{x}_B,\mathbf{x},\omega)$ is the Green's function in the actual state with a normal traction source and a normal particle velocity receiver at the free surface.

Before we show how $\hat{G}(\mathbf{x}_B,\mathbf{x},\omega)$ can be resolved from equation 3 by MDD, we discuss a way to extract the reference responses $\hat{\bar{v}}$ and $\hat{\bar{p}}$ from the observed passive data $\hat{v}(\mathbf{x}_B,\mathbf{x}_A,\omega)$. Assume that the subsurface consists of an inhomogeneous target below a relatively smooth overburden and that the source at $\mathbf{x}_A$ is located below the target. Assuming the source wavelet is a transient, the transmission response without free surface multiples, i.e., $\hat{\bar{v}}(\mathbf{x}_B,\mathbf{x}_A,\omega)$, can be estimated from the transmission response with free surface multiples, $\hat{v}(\mathbf{x}_B,\mathbf{x}_A,\omega)$, by applying a time window in the time domain and multiplying the result by one-half (to correct for the absence of the downgoing wavefield in the reference state). Both $\hat{\bar{v}}$ and $\hat{\bar{p}}$ are upgoing waves at the transparent surface $\partial\mathbb{D}_0$, so $\hat{\bar{p}}$ can be obtained from $\hat{\bar{v}}$ using a one-way wave equation for upgoing waves. For example, when $\partial\mathbb{D}_0$ is planar and the medium just below $\partial\mathbb{D}_0$ is laterally invariant, we can use the relation $\tilde{\bar{p}} = (\rho/q)\tilde{\bar{v}}$, where the tilde denotes the ray-parameter domain, ρ is the mass density, and q is the vertical slowness.

Next, we invert equation 3 for $\hat{G}(\mathbf{x}_B,\mathbf{x},\omega)$. In matrix notation (Berkhout, 1982), this equation can be written as

$$\hat{\mathbf{G}}\hat{\bar{\mathbf{P}}} = \hat{\mathbf{V}} - \hat{\bar{\mathbf{V}}} \tag{4}$$

(variables in boldface sans-serif font denote matrices containing discretized wavefields). A column of $\hat{\mathbf{V}}$ contains $\hat{v}(\mathbf{x}_B,\mathbf{x}_A,\omega)$ for a fixed source position $\mathbf{x}_A$ and variable receiver positions $\mathbf{x}_B$ (all for the same frequency component ω). Assuming responses $\hat{v}(\mathbf{x}_B,\mathbf{x}_A,\omega)$ are available for independent sources, they are stored in the different columns of $\hat{\mathbf{V}}$ [hence, a row of $\hat{\mathbf{V}}$ contains $\hat{v}(\mathbf{x}_B,\mathbf{x}_A,\omega)$ for a fixed receiver position $\mathbf{x}_B$ and variable source positions $\mathbf{x}_A$]. Matrices $\hat{\mathbf{G}}$, $\hat{\bar{\mathbf{P}}}$, and $\hat{\bar{\mathbf{V}}}$ are organized in a similar way.

The matrix equation can be solved per frequency component—for example, via weighted least-squares inversion—according to

$$\hat{\mathbf{G}} = (\hat{\mathbf{V}} - \hat{\bar{\mathbf{V}}})\mathbf{W}\hat{\bar{\mathbf{P}}}^{\dagger}(\hat{\bar{\mathbf{P}}}\mathbf{W}\hat{\bar{\mathbf{P}}}^{\dagger} + \epsilon^2\mathbf{I})^{-1}, \tag{5}$$

where the superscript † denotes transposition and complex conjugation, $\mathbf{W}$ is a diagonal weighting matrix, $\mathbf{I}$ is the identity matrix, and ϵ^2 is a stabilization parameter. The matrix $\mathbf{W}$ is used to compensate for large variations in the energy of the observed responses, whereas ϵ^2 prevents evanescent wave components from becoming unstable in the inversion. In general, $\mathbf{W}$ and ϵ^2 are frequency dependent. Applying the matrix inversion of equation 5 for each frequency component and transforming the result to the time domain is equivalent with MDD in the time domain.

With the actual sources only below a target area, the direct wave in $\hat{\mathbf{G}}(\mathbf{x}_B,\mathbf{x},\omega)$ will not be reconstructed properly. In practice $\hat{\mathbf{V}} - \hat{\bar{\mathbf{V}}}$ in equation 5 is, for convenience, replaced by $\hat{\mathbf{V}}$, causing another error in the direct-wave reconstruction. The erroneous direct-wave contribution is removed by muting the final result in the time domain.

Note that the matrix product $\hat{\mathbf{G}}\hat{\bar{\mathbf{P}}}$ in equation 4 is a discretized representation of the integral in the left-hand side of equation 3. This discretization assumes regular sampling of the receiver coordinate $\mathbf{x}$ in $\hat{\bar{p}}(\mathbf{x},\mathbf{x}_A,\omega)$. This is not a very severe assumption because the receivers are at the surface and their positions are known. In the case of irregular sampling, a regularization procedure (Duijndam et al., 1999) could be applied prior to MDD.

A more important observation is that MDD according to equation 5 can be carried out without knowing the source positions and the medium parameters (similar to crosscorrelation interferometry) and without assumptions with respect to the regularity of the source positions $\mathbf{x}_A$ (the latter property is unique for the MDD approach). Moreover, the MDD approach compensates for different types of sources, variations in power spectra, nonuniform radiation characteristics, and even spatially extended sources (e.g., plane-wave sources with different directions) because all of these effects are accounted for in the underlying equation 3. The quality of the MDD result depends mainly on the source density. An intuitive criterion is that the average horizontal distance between the sources should be smaller than half the minimum horizontal wavelength.

NUMERICAL EXAMPLE 1: IRREGULAR SOURCE DISTRIBUTION BELOW A TARGET

We illustrate the potential of MDD to account for irregular source distributions at the hand of 2D data modeled in a simple, horizontally layered, lossless medium.

Consider the configuration in Figure 2a, which consists of a horizontally layered target below a homogeneous overburden. The green triangles at the free surface denote 51 regularly spaced vertical geophones with $\Delta x_1 = 40$ m (only nine geophones are shown). The blue dots below the layered target denote 250 irregularly spaced sources with average $\Delta x_1 = 20$ m. These sources emit sequentially (in arbitrary order) transient acoustic waves. The central frequency of the sources is distributed randomly between 10 and 30 Hz. The responses are registered by the geophones at the surface, yielding 12,750 traces of 6 s, sampled with $\Delta t = 5$ ms. These are the passive data represented by $v(\mathbf{x},\mathbf{x}_A,t)$.

Figure 2b shows $v(\mathbf{x},\mathbf{x}_A,t)$ for fixed $\mathbf{x}_A$ (a subsurface source somewhere around $x_1 = 0$ m) and variable $\mathbf{x}$ (denoting the geophone positions at the surface). The time origin $t = 0$ in this figure does not need to correspond with the source action; any source time shift is removed in the subsequent correlation or deconvolution process.

First, we apply seismic interferometry (Green's function retrieval) by crosscorrelation. For a fixed (but unknown) source position $\mathbf{x}_A$, we crosscorrelate the trace at the central receiver ($\mathbf{x} = 0$) with the traces at all other receivers. We repeat this for all sources and sum the result per receiver over all sources. The causal part of the result is an estimate of the reflection response (the Green's function) at all receivers at the free surface, resulting from a source at $\mathbf{x} = 0$ and $t = 0$. By time reversing the acausal part and adding this to the causal part (to improve the signal-to-noise ratio, or S/N), we obtain the result shown by the red traces in Figure 2c (only every fifth trace is shown). The black dashed traces in this figure represent the directly modeled reflection response. Note that the arrival times of the interferometric result nicely match those of the directly modeled result, but the waveforms and amplitudes are not accurately reconstructed. Moreover, the interferometric results are somewhat noisy because of the irregularities in the source distribution and the variations in the source spectra.

Next, we apply interferometry by MDD, as discussed in the previous section. The first arrivals (including internal multiple scattering in the target) in $v(\mathbf{x},\mathbf{x}_A,t)$ are well separated in time from the surface-related multiples, so the reference response $\bar{v}(\mathbf{x},\mathbf{x}_A,t)$ is extracted

easily by applying a time window, indicated by the dashed box in Figure 2b. Then $\bar{p}(\mathbf{x},\mathbf{x}_A,t)$ is approximated by multiplying $\bar{v}(\mathbf{x},\mathbf{x}_A,t)$ with $\rho c/\cos\alpha(\mathbf{x})$, where c is the propagation velocity of the overburden and $\alpha(\mathbf{x})$ is the angle between the propagation direction of the first arrival at $\mathbf{x}$ and the normal at the surface [this angle can be estimated from the local time dip of $\bar{v}(\mathbf{x},\mathbf{x}_A,t)$].

In the next step, v and $\bar{p}$ are Fourier transformed and stored in matrices $\hat{\mathbf{V}}$ and $\hat{\bar{\mathbf{P}}}$, which are created for each frequency component. The Green's matrix $\hat{\mathbf{G}}$ is obtained by applying equation 5 (with $\hat{\mathbf{V}} - \hat{\bar{\mathbf{V}}}$ replaced by $\hat{\mathbf{V}}$). Using source-receiver reciprocity, we add the transpose of $\hat{\mathbf{G}}$ to improve the S/N. Taking the central column and applying an inverse Fourier transform gives $G(\mathbf{x}_B,\mathbf{O},t)$ for variable $\mathbf{x}_B$. This Green's function is represented by the red traces in Figure 2d (every fifth trace is shown); the black dashed traces in this figure represent the directly modeled result (results have been convolved with the same wavelet). Arrival times, waveforms, and amplitudes match very well, and the noise level is significantly lower than in Figure 2c.

NUMERICAL EXAMPLE 2: SOURCES SANDWICHED BETWEEN LAYERS

One of the underlying assumptions of MDD is that the reference response $\bar{v}(\mathbf{x},\mathbf{x}_A,t)$ can be separated from the observed passive data $v(\mathbf{x},\mathbf{x}_A,t)$. This is not always possible by time windowing because of interference of later arrivals in $\bar{v}(\mathbf{x},\mathbf{x}_A,t)$ with, for example, the surface-related multiples in $v(\mathbf{x},\mathbf{x}_A,t)$. What we can do in such cases is to ignore the later arrivals and approximate $\bar{v}(\mathbf{x},\mathbf{x}_A,t)$ by the first arrival in $v(\mathbf{x},\mathbf{x}_A,t)$ (including the short-period internal multiples). Following this procedure, equation 5 still retrieves the main reflection events in the Green's function correctly, but it will also result in spurious events. In the following example, we show that, in specific situations, these spurious events may disappear.

We consider the same configuration as in Figure 2a but with one reflector added at depth level $x_3 = 2400$ m, which is below the sources. Figure 3a shows the response of one of the sources. The true reference response $\bar{v}(\mathbf{x},\mathbf{x}_A,t)$ now also contains reflections from this deeper reflector, but we approximate it by extracting the first arrival from $v(\mathbf{x},\mathbf{x}_A,t)$ (indicated by the dashed box in Figure 3a). The reference response $\bar{p}(\mathbf{x},\mathbf{x}_A,t)$ is obtained in the same way from $\bar{v}(\mathbf{x},\mathbf{x}_A,t)$ as in the previous example (hence, it also contains only the first arrival).

For the first experiment in this model, we consider sources that are perfectly aligned at depth level $x_3 = 1400$ m. The result of interferometry by MDD is shown in Figure 3b and is compared with the directly modeled response (a larger portion of the time axis is shown than in Figure 2). We see a good match for the main events, but we

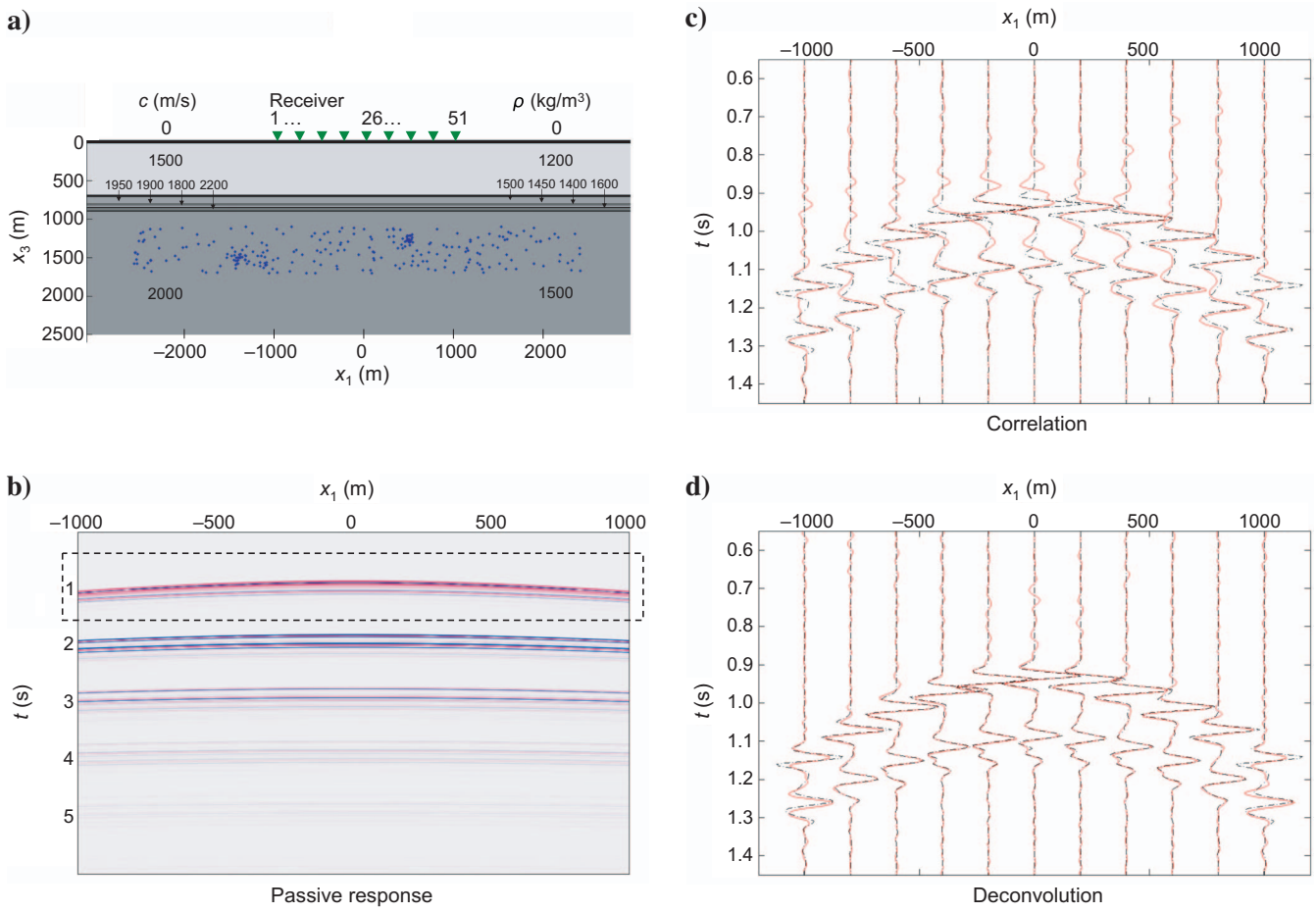

Figure 2. Numerical example of seismic interferometry with irregular sources. (a) Configuration with a horizontally layered target below a homogeneous overburden and a free surface. The irregularly distributed sources below the target emit transient signals sequentially. (b) Response of one of the sources. (c) Result of interferometry by crosscorrelation (red traces) compared with the directly modeled response of a source at $\mathbf{x} = \mathbf{O}$ (black dashed traces). (d) Result of interferometry by MDD.

also see a spurious event (indicated by the arrow) interfering with the target response because of the approximations in $\bar{v}$ and $\bar{p}$ (this spurious event can be interpreted as the result of the deconvolution of the reflected wave by the first arrival).

We repeat the experiment with the same model but this time with the irregular source distribution of Figure 2a. The result is shown in Figure 3c. The spurious event completely disappears, but all other events (including the response of the reflector below the sources) remain untouched. The randomness of the source depths destroys the coherency of the spurious event related to the reflector below the sources. Draganov et al. (2004) first discussed this effect for the crosscorrelation method.

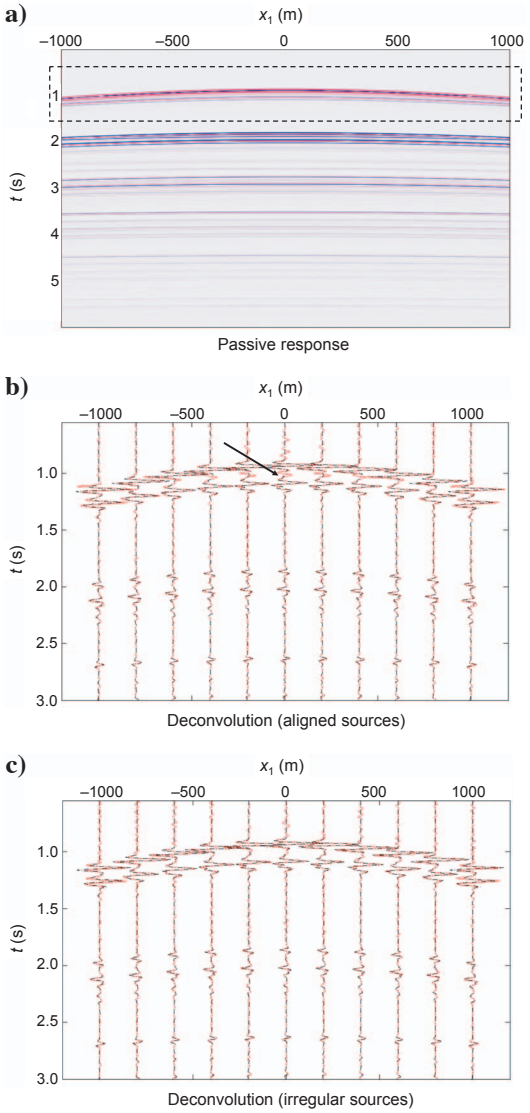

Figure 3. Numerical example for the configuration of Figure 2a, with an extra reflector below the sources. (a) Response of one of the sources. (b) Result of interferometry by MDD when the sources are aligned at a constant depth. Note the spurious event in the target response. (c) Result of interferometry by MDD with irregularly distributed sources. Note the absence of spurious events.

REVISITING THE ELASTODYNAMIC SITUATION

We indicate the required modifications for applying MDD to the elastodynamic situation. Equation 2 is an exact implicit representation for the elastodynamic Green's function $\hat{G}_{mj}(\mathbf{x}_B, \mathbf{x}, \omega)$ in an arbitrary inhomogeneous anisotropic dissipative medium. Similar to the acoustic situation, the main complication for resolving $\hat{G}_{mj}$ is that the reference responses $\hat{\bar{v}}_m$ and $\hat{\bar{t}}_j$ must be extracted from the observed data $\hat{v}_m(\mathbf{x}_B, \mathbf{x}_A, \omega)$. Assuming transient sources, we propose to (1) decompose the particle velocity data at the free surface into upgoing (quasi-) P- and S-waves, (2) extract the first arrivals to obtain an approximation of the P and S reference responses, and (3) recompose these responses into the reference particle velocity $\hat{\bar{v}}_m$ and traction $\hat{\bar{t}}_j$. The effect of the approximations in $\hat{\bar{v}}_m$ and $\hat{\bar{t}}_j$ on the retrieved Green's function remains to be investigated.

Another issue is that equation 2 has the appearance of three equations ($m = 1,2,3$) for nine unknown Green's functions $\hat{G}_{mj}$. Solving this apparent ill-posedness requires that there be multiple types of sources in the subsurface (e.g., forces in different directions) in addition to many source positions. Note that the different types of sources do not need to share the same positions.

CONCLUSIONS

We propose passive seismic interferometry by MDD as an alternative to the crosscorrelation method. The main advantage of MDD is its relative insensitivity to irregular source distributions. Moreover, it can be applied to dissipative media. The main complication is the underlying assumption that the reference response can be separated from the observed data. We have discussed the application for sequentially recorded responses of transient sources in configurations for which the surface-related multiples do not interfere significantly with the first arrival. When these assumptions are fulfilled only partially, MDD still recovers the main events accurately but spurious events appear as well. However, spurious events related to reflectors below the sources are largely suppressed because of the randomness of the source positions.

Unlike in the crosscorrelation method, in MDD the responses at all receivers are involved simultaneously in the matrix inversion. This matrix inversion makes MDD more costly than crosscorrelation. Moreover, it requires a regular receiver grid, or at least a grid that is dense enough to allow regularization.

The choice for applying passive seismic interferometry by crosscorrelation or by MDD depends on many factors. In some cases, it may be useful to use a hybrid approach of MDD and crosscorrelation. Because the crosscorrelation method does not rely on the separation of the first arrival, it can be used to identify which events in the MDD result are actual reflections and which are spurious events. Despite the underlying assumptions of MDD, we believe its relative insensitivity for irregularities in the source distribution makes it an attractive approach for various applications, ranging from reservoir imaging and characterization using microseismic data to crustal imaging with teleseismic data.

ACKNOWLEDGMENTS

This work is supported by The Netherlands Research Centre for Integrated Solid Earth Science (ISES); The Netherlands Organisation for Scientific Research (NWO, Toptalent 2006 AB); and the Dutch Technology Foundation (STW), an applied science division

of NWO and the technology program of the Ministry of Economic Affairs (grant DCB.7913). We thank the associate editor (Paul Sava) and three reviewers (Dirk-Jan van Manen, Roel Snieder, and Xander Campman) for their constructive comments, which improved the quality of this paper.

REFERENCES

Aki, K., and P. G. Richards, 1980, Quantitative seismology: W. H. Freeman & Company.

Amundsen, L., 1999, Elimination of free surface-related multiples without need of the source wavelet: 69th Annual International Meeting, SEG, Expanded Abstracts, 1064–1067.

Berkhout, A. J., 1982, Seismic migration: Imaging of acoustic energy by wave field extrapolation: Elsevier Science Publ. Co., Inc.

Draganov, D., K. Wapenaar, and J. Thorbecke, 2004, Passive seismic imaging in the presence of white noise sources: The Leading Edge, **23**, 889–892.

Duijndam, A. J. W., M. A. Schonewille, and C. O. H. Hindriks, 1999, Reconstruction of band-limited signals, irregularly sampled along one spatial direction: Geophysics, **64**, 524–538.

Malcolm, A. E., J. A. Scales, and B. A. van Tiggelen, 2004, Extracting the Green function from diffuse, equipartitioned waves: Physical Review E, **70**, 015601(R).

Mehta, K., R. Snieder, and V. Graizer, 2007, Extraction of near-surface properties for a lossy layered medium using the propagator matrix: Geophysical Journal International, **169**, 271–280.

Schuster, G. T., and M. Zhou, 2006, A theoretical overview of model-based and correlation-based redatuming methods: Geophysics, **71**, no. 4, SI103–SI110.

Snieder, R., J. Sheiman, and R. Calvert, 2006, Equivalence of the virtual-source method and wave-field deconvolution in seismic interferometry: Physical Review E, **73**, 066620.

Snieder, R., K. Wapenaar, and U. Wegler, 2007, Unified Green's function retrieval by cross-correlation: Connection with energy principles: Physical Review E, **75**, 036103.

Wapenaar, C. P. A., and D. J. Verschuur, 1996, Processing of ocean bottom data: The Dolphin Project: Delft University of Technology, 6.1–6.26, http://www.ta.tudelft.nl/PrivatePages/C.P.A.Wapenaar/Daylight2/Delp_96G.pdf.

Wapenaar, K., D. Draganov, and J. Robertsson, eds., 2008a, Seismic interferometry: History and present status: SEG.

Wapenaar, K., E. Slob, and R. Snieder, 2008b, Seismic and electromagnetic controlled-source interferometry in dissipative media: Geophysical Prospecting, **56**, 419–434.